# DESIGN AND EXPERIMENT OF A HYDRAULIC DRIVE SYSTEM FOR A TRACKED TOBACCO HARVESTER BASED ON DUAL-VARIABLE PUMP-MOTOR COORDINATED CONTROL

/

# 基于·双变量泵控马达协同控制的履带式烟草收获机液压行走系统设计与试验

**Chenhui ZHU[1)], Bingjie CHEN [1)], Bo LUO[1,2)], Zijian LI [1)], Bingjie LIU [3*)]**

[1)]College of Mechanical and Electrical Engineering, Henan Agricultural University, Zhengzhou 450002 / China

[2)]School of Intelligent Engineering, Zhengzhou College of Finance and Economics, Zhengzhou 450000 / China

[3)]College of Information and Management Science, Henan Agricultural University, Zhengzhou 450002 / China

*Corresponding author: Bingjie Liu*

*Tel: +8615038352581; E-mail of corresponding author: liubingjie@henau.edu.cn*

*DOI: https://doi.org/10.35633/inmateh-77-42*

***Keywords:*** *Tracked type; Double pump-double motor; Fuzzy PID; Cross-coupling*

## ABSTRACT

*To address the insufficient driving stability of dual-pump dual-motor hydraulic systems in tracked tobacco harvesters, this study proposes a dual-mode cooperative control strategy comprising straight-line and steering modes. In the straight-line mode, a cross-coupled fuzzy PID synchronization control layer is integrated into the existing single-channel fuzzy PID speed control loop. This configuration enforces synchronous operation of the two motors and significantly enhances speed tracking accuracy. In the steering mode, an inner-track deceleration differential control scheme is implemented to reduce the speed of the inner crawler, thereby achieving smoother turning motion. Cement pad tests were conducted to evaluate the performance of the proposed control strategy. The experimental results indicate that, compared with the conventional PID control strategy, the single-channel fuzzy PID control strategy reduces the steady-state error during straight-line motion by 46%–70%. Furthermore, the dual-loop fuzzy PID control strategy incorporating the cross-coupled synchronization layer decreases the steady-state error by 62% relative to the parallel PID control strategy. Overall, the proposed controller provides a robust control solution for dual-pump dual-motor hydraulic drive systems and offers a valuable reference for the development of high-performance tracked agricultural vehicles.*

## 摘要

*该研究针对履带式烟草收获机双泵-双马达液压驱动系统行驶稳定性差的问题，提出一种“直线-转向”双工况的协同控制新方法。直线行驶时，在单通道液压马达模糊 PID 控制器基础上引入交叉耦合模糊 PID 同步策略，实现双马达转速同步输出，显著提升直线作业的稳定性与精度；转向时采用内侧减速差动转向模式，通过主动降低内侧履带速度实现平稳转弯。水泥硬路面试验表明：与传统 PID 相比，模糊 PID 控制较常规 PID 在直线行驶稳态误差上降低 46%至 70%，双闭环模糊 PID 较并行式 PID 误差减少 62%，该方法增强了整机行驶稳定性与准确性，为双泵-双马达液压驱动系统提供了可靠解决方案，为推动高效农业装备发展提供了参考。*

## INTRODUCTION

At present, the transmission system of fully hydraulic crawler vehicles generally adopts the transmission form of variable displacement pump + fixed displacement motor or variable displacement pump + variable displacement motor. To address the control challenges of the hydraulic transmission system in crawler vehicles, precise control of the hydraulic motor speed has become an urgent issue. The control of the hydraulic motor speed directly impacts the working efficiency of the equipment and is also related to the stability and safety of the system. Therefore, studying the motor speed control of the hydraulic transmission system is of great significance for enhancing the overall system performance.

In recent years, a large number of experts and scholars at home and abroad have carried out extensive research on the speed control method of pump-motor transmission technology in full hydraulic tracked vehicles. S Fu et al. effectively improved the work efficiency of the excavator based on the positive flow control system of the electric excavator with variable speed control *(Fu S., 2020)*.

The direct-drive hydraulic system with adaptive nonlinear pump flow compensation proposed by Helian B et al. achieved precise motion control *(Helian B., 2020)*. *Pascal M.A., (2020),* focused on the nonlinear PID actuator speed control in inverter-based electro-hydraulic systems, considering the influence of external leakage on the system. The advanced valve and pump coordinated hydraulic control design proposed by *Lyu et al, (2020),* optimized the operation of the hydraulic system, improving its efficiency and stability. The speed control system of the dual-variable hydraulic transformer developed by *Shen W. et al., (2022),* uses an intelligent control algorithm to monitor the pressure and flow of the hydraulic system in real time, dynamically adjusting these two variables according to the set speed target to achieve the desired speed and efficiency requirements. *Ranjan P. et al., (2020)*, explored the problem of motor speed control in hydraulic transmission systems from a different perspective with their new method for energy recovery and position control of hybrid hydraulic excavators. *Wrat G. et al., (2020)*, proposed a method for energy saving in electro-hydraulic systems by leakage compensation through proportional flow control valves. Utilizing a fuzzy-PID position control strategy, they effectively improved the energy efficiency of the system. *Tian Q., (2021),* studied the extraction of instantaneous speed fluctuations and their application in the evaluation of hydraulic system efficiency, providing theoretical support for the optimization of hydraulic system efficiency. *Duan Z. et al, (2024),* studied the servo valve-controlled hydraulic motor system based on an active disturbance rejection control strategy, effectively improving the control accuracy and stability of the system. *Wang J. et al, (2023),* proposed a nonlinear model predictive control method based on hydraulic motor speed mapping for the trajectory tracking control problem of skid-steering mobile robots. This method achieves precise tracking of the mobile robot's trajectory by adjusting the speed of the hydraulic motor in real time, providing a new solution for the control of mobile robots. In terms of robustness, *Nguyen M.H., (2023),* studied the output feedback robust tracking control of variable speed pump-controlled hydraulic systems under mismatched uncertainties. Using robust control theory, they developed a novel control method that successfully enhanced the system's tracking and stability under unpredictable circumstances. The application of electro-hydraulic systems in complicated situations is theoretically supported by this research. By lowering the size of the electric motor in electric mobile machinery, *Wang F.*, *(2023),* proposed a power-sharing electro-hydraulic actuator system that achieves efficient power consumption. *Zhang X., (2023),* investigated the design and optimization of a self-compensating oil distributor for hydraulic motors, successfully enhancing the motor's reliability and overall performance. In order to optimize system parameters and increase performance, *Lu S., (2023),* introduced the gray wolf particle swarm optimization algorithm to the pump-motor servo system's constant speed control approach. This research provides a new method for the optimal control of electro-hydraulic systems.

In recent years, relevant experts and scholars have conducted in-depth research on the problem of dual -axis synchronization control of the hydraulic system *(Liao L. et al., 2023)*. *Cao Yang, (2023),* discussed the performance characteristics and application of hydraulic synchronous system in detail, discussed the causes of its operation error, and gave the corresponding treatment strategy. *Xie Jinhui, (2013),* modeled the dual hydraulic motor synchronous drive system on the basis of certain simplified assumptions, and used the synchronous closed-loop position feedback PID control method for the motor speed output, and used the double-motor angular displacement difference as a parameter to perform closed-loop feedback on the hydraulic system. This method improves the synchronization performance of the hydraulic system. *Liu et al., (2022),* studied the hydraulic pin-type lifting system of a jack-up wind power installation vessel, which is a two-stage hydraulic synchronous control system. To improve the synchronization accuracy, a speed tracking and displacement coupling synchronous control strategy was adopted for the single pile leg, and a fuzzy PID control algorithm was used to enhance the robustness of the system. *Zhao et al., (2022),* developed a fuzzy PID controller based on particle swarm optimization to address synchronization errors caused by uneven stress in the friction and new hydraulic fan brake drive cylinder group. *Fang et al., (2020),* implemented fuzzy PID control in the C32 hydraulic servo system, thereby increasing the welding process's closed-loop control characteristics. *Wang et al., (2022),* developed a neural network-based synchronous controller to alleviate the synchronization error induced by the difficulty of coordinated operation in hydraulic multi-actuator synchronous systems.

Based on prior research, a control strategy for the drive system of a tracked tobacco harvester was developed to address the insufficient driving stability of the dual-pump dual-motor hydraulic drive system. For straight-line motion, a cross-coupled fuzzy PID synchronous control method is proposed to ensure coordinated operation of the two motors. For steering control, an inner-track deceleration differential steering mode is adopted. The proposed control strategy significantly enhances the stability and tracking accuracy of the tracked tobacco harvester.

## MATERIALS AND METHODS

### *Design of the Hydraulic Drive System for a Tracked Tobacco Harvester*

#### *The structure of Tracked Tobacco Harvester*

Tracked tobacco harvester is a kind of self-propelled operating machine designed for hilly areas. Its main design parameters are shown in Table 1. Its structure is mainly composed of crawler drive chassis, frame, cab, tobacco harvesting and conveying device, tobacco picking frame, hydraulic power system and corresponding control system. As shown in Fig. 1, the gantry frame structure is adopted to ensure its passing ability in the field and reduce the damage to tobacco leaves during operation.

**Table 1**

**Main design parameters of the tracked tobacco harvester**

| Parameter | Value | Unit |
|---|---|---|
| **Overall dimensions (L × W × H)** | 4.30×1.78×3.20 | m |
| **Machine mass** | Approximately 4000 | kg |
| **Track width** | 1.46 | m |
| **Track gauge (center-to-center distance)** | 1.5 | m |
| **Track pitch** | 0.22 | m |
| **Ground clearance** | 0.28 | m |
| **Ground contact pressure** | 0.05 | MPa |
| **Drive sprocket radius** | 0.158 | m |
| **Track ground contact length** | 2.80 | m |

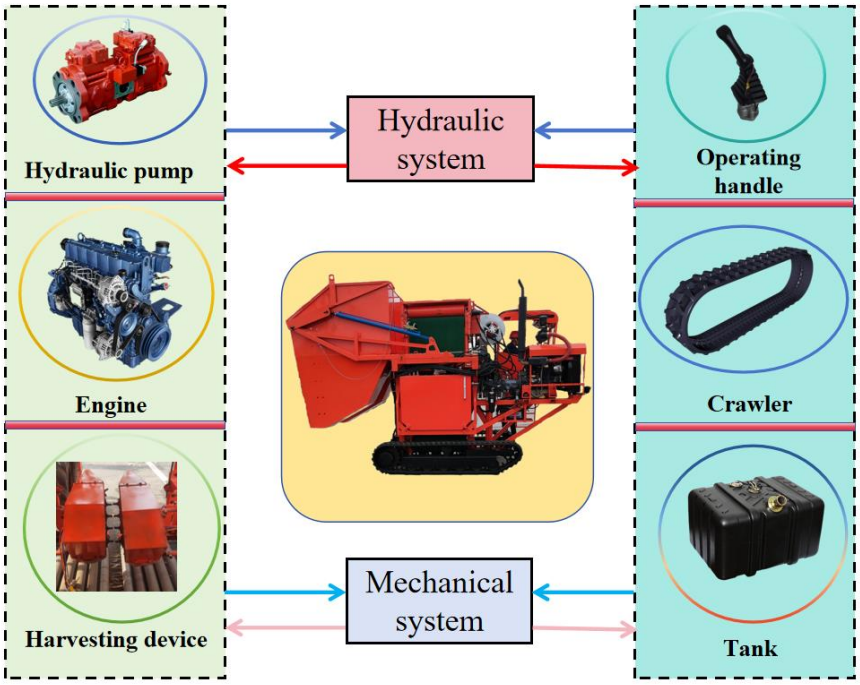


**Fig. 1 - Schematic diagram of tracked tobacco harvester**

*1. Cab; 2. Engine; 3. Picking device; 4. Drying frame; 5. Hydraulic oil tank; 6. Tracked chassis; 7. Conveyor*

### *Working Principle of the Hydraulic Drive System of the Tracked Tobacco Harvester*

The hydraulic drive system of the tracked tobacco harvester adopts a dual-variable displacement pump–dual fixed-displacement motor configuration. Figure 2 illustrates the hydraulic system used to control the pumps. This drive system enables independent bilateral track operation, and its performance is less affected by interference between hydraulic circuits. As a result, it allows for easy and precise control of the various driving functions of the tracked vehicle.

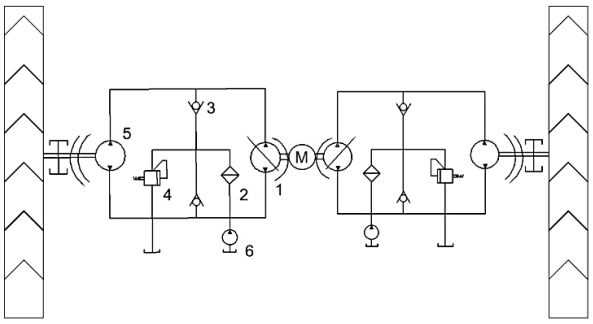


**Fig. 2 - Pump-controlled hydraulic motor system of the tracked tobacco harvester.**
*1. Variable pump; 2. Filter; 3. Check valve; 4. Relief valve; 5. Hydraulic motor; 6. Charge pump*

During operation, the engine output power is transmitted through the coupling directly to the dual variable-displacement pumps, which then drive the hydrostatic transmission systems on both sides of the harvester. The actuators of the hydrostatic transmission are Likechuan fixed-displacement reduction hydraulic motors. By adjusting the displacement of the two variable pumps via the drive system controller, the output speed of the travel motors can be continuously regulated, thereby controlling the harvester's traveling speed.

The drive system of the tobacco harvester is powered by two fixed-displacement reduction travel motors. During operation, these motors drive the sprockets on both sides of the machine, enabling forward motion. Owing to external disturbances, the loads acting on the left and right sides vary continuously in real time. To ensure stable operation of the harvester on uneven or sloped terrain, the output speeds of the two travel motors must be precisely regulated, thereby enabling accurate and stable control of the machine's motion.

***Design of a Drive System Control Method for a Tracked Tobacco Harvester***

The key to achieving precise and stable straight-line and steering motions of the harvester lies in maintaining stable speeds of the tracked motors on both sides. Therefore, for the single-channel pump-controlled motor system of the tracked tobacco harvester, an effective speed control strategy is required to mitigate the influence of external load fluctuations on motor speed. After stable speed regulation is achieved in the single-channel system, appropriate coordinated control strategies are then implemented for the dual-channel pump-controlled motor system to accurately accomplish straight-line driving and steering maneuvers.

***Single-Channel Variable-Pump–Motor Stable Speed Control Method***

During straight-line operation of the tobacco harvester, frequent acceleration and deceleration, as well as continuous variations in external load, can disturb the output speed of the hydraulic motor. Similarly, during steering, changes in steering resistance further affect the stability of the motor speed. To address these challenges, the single-channel variable-pump–motor system of the tobacco harvester requires a control method with strong anti-disturbance capability and high stability. In addition, to accommodate step inputs associated with gear shifting, the control algorithm must exhibit fast dynamic response and minimal overshoot.

***Design of Fuzzy Adaptive PID Controller***

The single-channel pump-controlled motor system of the tobacco harvester employs a fuzzy adaptive PID control algorithm to regulate the output speed of the hydraulic motor. To achieve accurate and stable speed control under varying operating conditions, the parameters of the fuzzy PID controller must be dynamically adjusted. As illustrated in Figure 3, in the fuzzy control mode, the speed deviation ( e ) and the rate of deviation change ( ec ) serve as input variables, while the adjustments to the PID parameters ( $\Delta K_P$ ), ( $\Delta K_I$ ), and ( $\Delta K_D$ ) act as output variables. The controller continuously evaluates and analyzes the values of the input errors ( e ) and ( ec ), and then adjusts the parameters ( $K_P$ ), ( $K_I$ ), and ( $K_D$ ) based on predefined fuzzy reasoning rules to achieve the desired control performance *(Ren Q. et al., 2020)*.

In the fuzzy control system, the fuzzy controller plays a critical and direct role in determining control performance *(Ren H., Li W., Ye S. et al., 2023)*. The Mamdani method, known for its intuitiveness, ease of implementation, and ability to incorporate manual input, has been widely adopted in control applications *(Senthilkumar P. et al., 2023)*. This section employs the Mamdani fuzzy reasoning method to dynamically adjust the PID parameters. The input and output fuzzy sets are defined as {NB, NM, NS, ZE, PS, PM, PB}, and triangular membership functions are used to fuzzify the input variables, ensuring adaptability to the system's nonlinear characteristics and dynamic changes.

The program design flowchart of the fuzzy PID controller for the tracked tobacco harvester is depicted in Figure 3. The controller dynamically adjusts the PID parameters in real-time based on the deviation and deviation rate between the target speed and the actual speed of the hydraulic motor. Specifically, when the deviation is large, the proportional gain ( $K_P$ ) is increased to enhance the system's response speed, while the integral gain ( $K_I$ ) is reduced to prevent integral saturation and overshoot. Conversely, when the deviation is small, ( $K_P$ ) and ( $K_I$ ) are decreased to minimize system overshoot and eliminate steady-state error. The differential parameter ( $K_D$ ) is adjusted according to the rate of deviation change to provide appropriate damping, thereby avoiding excessive overshoot or oscillation during the dynamic process. Defuzzification is performed using the centroid method to ensure smooth output and efficient utilization of information, enabling precise adjustment of the PID parameters.

Finally, the PID controller converts the speed deviation signal into an analog voltage signal, which is input to the pump-controlled motor speed regulation system. This signal adjusts the displacement of the electrohydraulic proportional variable pump, thereby regulating the rotational speed of the hydraulic motor and enabling precise control of the pump-controlled motor system of the tracked tobacco harvester under various operating conditions.

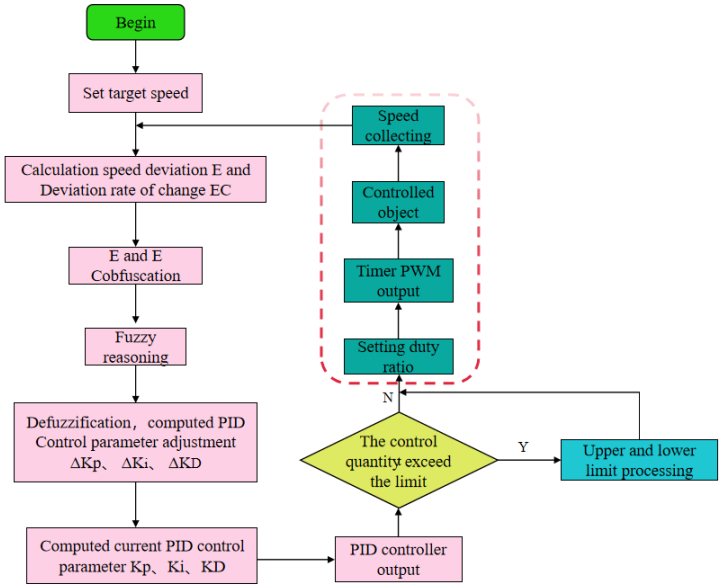


**Fig. 3 - Fuzzy PID controller programming flowchart**

### *Design of a Control Method for the Drive System of a Tracked Tobacco Harvester*

To achieve precise control of the harvester, it is essential to ensure accurate execution of its two fundamental driving motions: straight-line travel and steering. Given the dual-pump dual-motor configuration of the tracked tobacco harvester's drive system, the control challenges under these two operating conditions involve both the stable speed regulation of the single-channel pump-controlled motor system and the coordinated control of the dual-channel pump-controlled motor system.

### *Straight-Line Driving Control Method of the Tracked Tobacco Harvester*

Straight-line driving is the most fundamental motion of the tobacco harvester. In the dual-pump dual-motor drive control system, when identical control currents are applied to the variable-displacement pumps on both sides, the travel motors are theoretically expected to produce the same output speed. However, in practice, discrepancies arise due to variations in the machining accuracy of hydraulic components, manufacturing asymmetries of the harvester structure, non-centered mass distribution, and the complex operating conditions encountered in hilly and mountainous terrain. These factors lead to differences in the rotational speeds of the left and right tracks, which can cause the vehicle to deviate from its intended straight-line trajectory.

The tracked tobacco harvester employs a fuzzy adaptive PID closed-loop control strategy for its single-channel variable pump–controlled motor system, which effectively suppresses load disturbances and ensures stable output of the single-channel travel motor speed. However, when the left and right tracks are subjected to significantly different loads—such as during sudden terrain changes—the output speeds of the dual-channel travel motors may experience abrupt deviations.

In such cases, coordinated dual-channel control is required to minimize the instantaneous speed difference between the two sides. In classical dual-axis synchronous control of hydraulic systems, cross-coupled closed-loop synchronous control is widely used to mitigate mismatches between channels caused by external disturbances. This method improves the control accuracy of each channel by introducing coupling feedback between them, thereby enhancing synchronization performance. The schematic diagram of this control structure is shown in Figure 4. The cross-coupled synchronous control treats the two travel motor channels as an integrated system, which is more consistent with the linear motion control requirements of the tracked tobacco harvester. To achieve stable straight-line motion in hilly tobacco fields, the single-channel pump-controlled motor system adopts a fuzzy adaptive PID closed-loop control method, while the dual-channel pump-controlled motor system employs a dual-loop composite control strategy based on cross-coupled synchronous closed-loop control.

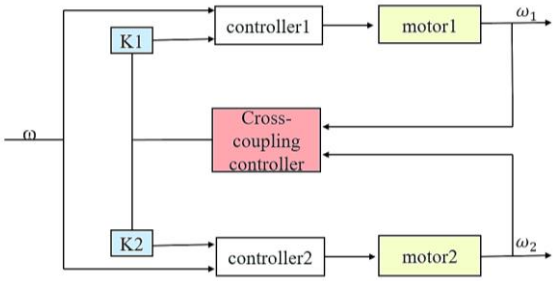


**Fig. 4 - Cross-coupled closed-loop synchronization control**

***Straight-Line Driving Control Logic Design of the Tobacco Harvester***

When the tracked tobacco harvester operates in a straight line in hilly tobacco fields, $n_1$ and $n_2$ denote the rotational speeds of the hydraulic motors on the left and right sides, respectively, and $n_k$ represents the speed difference between the two motors. The parameter $e$ is defined as the allowable straight-line deviation threshold. When $n_k < e$, the controller does not take corrective action, and the system continues operating normally. When $n_k \geq e$, the controller activates the dual closed-loop straight-line driving control program of the tracked harvester. The flowchart of the straight-line driving control logic is shown in Figure 5. By accelerating the lower-speed channel and decelerating the higher-speed channel, the output speeds of the two channels are gradually synchronized. This coordinated adjustment ultimately ensures equalized motor speeds on both sides, thereby enabling stable straight-line motion of the tracked tobacco harvester.

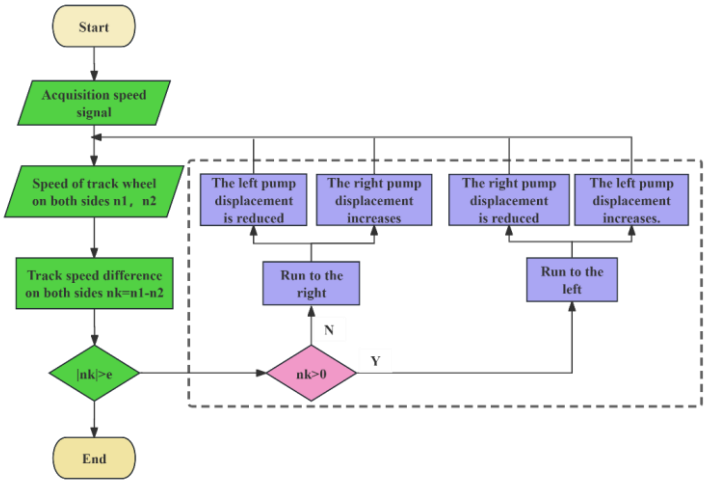


**Fig. 5 - Straight-line driving control flowchart of the tracked tobacco harvester**

***Steering Control Method of the Drive System of the Tracked Tobacco Harvester***

The tracked tobacco harvester achieves steering by regulating the relative speeds of the tracks on both sides. By adjusting the output speeds of the travel motors in the left and right track channels, a speed differential is generated, which produces the turning motion of the vehicle. Currently, the most commonly used steering modes for tracked vehicles include central differential steering, inner-track deceleration steering, and outer-track acceleration steering. The corresponding kinematic relationships for these steering modes are expressed as follows:

$$V_1 = V_0 \quad V_1' = 0 \tag{1}$$

$$R = \frac{V_1}{\omega} - \frac{B}{2} \tag{2}$$

$$R' = -\frac{V_0 \omega'}{\omega^2} \tag{3}$$

where: $R$ - is the steering radius of the tracked vehicle, m;
$\omega$ - is the steering angular velocity, rad/s;
$V_1$ - is the speed of the outer track, m/s;
$V_2$ - is the speed of the inner track, m/s;
$B$ - is the center-to-center distance between the two tracks, m.

When the tracked harvester performs a turning maneuver, its motion can be decomposed into a translational motion and a rotational motion about the instantaneous center of rotation C. The speed difference between the left and right tracks is the fundamental condition for realizing vehicle steering. When the two tracks move at the same speed and in the same direction, the vehicle travels in a straight line. When the two tracks move at equal speeds but in opposite directions, the tracked vehicle performs an in-place turn. According to the force conditions acting on the two tracks under different turning radii, steering can be classified into two modes: R ≥ B/2 and 0 ≤ R < B/2. The corresponding steering configurations are illustrated in Figure 6.

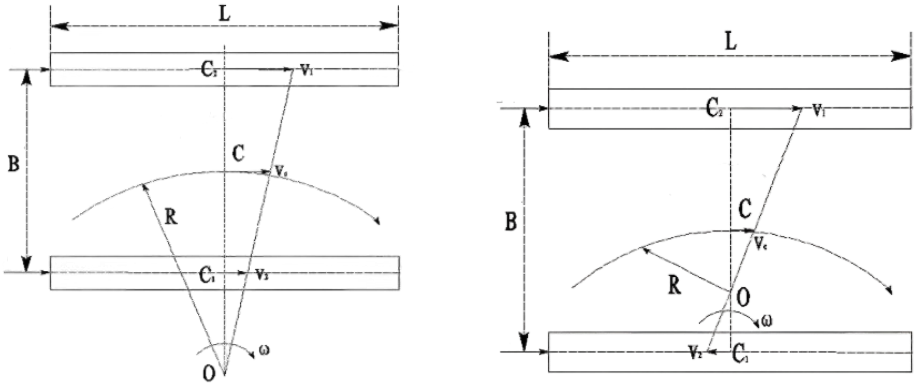


**(a) (R≥B/2)** **(b) (0≤R＜B/2)**

**Fig. 6 - Schematic diagram of tracked vehicle steering**

**Table 2**

**Tracked Vehicle Parameters**

| No. | Symbol | Parameter |
|---|---|---|
| 1 | $V_1$, $V_2$ | Inner and outer track speeds (m/s) |
| 2 | $V_c$ | Center speed (m/s) |
| 3 | $R$ | Steering radius (m) |
| 4 | $\omega$ | Steering angular velocity (rad/s) |
| 5 | $B$ | Track gauge (m) |
| 6 | $L$ | Track base (m) |
| 7 | $C$, $C_1$, $C_2$ | Vehicle center, inner-track center, and outer-track center of rotation |
| 8 | $O$ | Instantaneous turning center |
| 9 | $G$ | Gravitational force (N) |
| 10 | $\mu$ | Steering resistance coefficient |
| 11 | $f$ | Ground deformation resistance coefficient |
| 12 | $J$ | Moment of inertia |

The definitions of the parameters indicated in the diagram are provided in Table 2. When the tobacco harvester adopts the inner-track deceleration steering mode, it is initially assumed to move in a straight line at a constant speed $V_0$. During steering, the operator inputs a right-turn command via the speed control handle. Consequently, the left track maintains its speed at $V_1$, while the speed of the right track is reduced to $V_2$. According to the steering kinematic relationships of tracked vehicles, the following expressions can be derived:

$$V_2 = \frac{2R - B}{2R + B} V_0 \tag{4}$$

$$\omega = \frac{2V_C}{2R + B} \tag{5}$$

Similarly, when the tobacco harvester executes a turning maneuver with a specified steering radius, the corresponding kinematic equations of the tracked vehicle can be expressed as follows:

$$V_2 = \frac{B - 2R}{B + 2R} V_0 \tag{6}$$

$$\omega = \frac{2V_C}{2R + B} \tag{7}$$

During operation, the speed and direction of the tracked tobacco harvester are controlled by the coordinate input signal (x, y) from the speed control handle. Based on the real-time values of (x, y), the controller calculates the desired rotational speeds and directions of the left and right travel motors. The controller then generates corresponding PWM signals to regulate the displacement and rotation direction of the variable-displacement pumps. By adjusting the pump outputs, the speeds and directions of the tracks on both sides of the harvester are controlled, thereby enabling accurate steering and maneuvering.

***Driving Test of Tracked Tobacco Harvester***

The driving process of the tracked vehicle can be decomposed into two states: straight-line driving and steering. In this chapter, basic tests for straight-line driving and steering of the tracked tobacco harvester were conducted on a cement hard road surface. In the experiments, the driving control method and its program for the tobacco harvester were verified.

***Tracked Tobacco Harvester Straight Line Driving Performance Test***

Straight line driving is one of the important basic functions of tracked tobacco harvester. In this section, the difference between PID and fuzzy PID on the precise speed output control of single-channel pump-controlled motor is compared and analyzed in the straight-line walking test. At the same time, the effect of cross-coupled dual-motor speed synchronization control when the harvester is running in a straight line is verified.

***Test Scheme Design and Implementation Method***

Four control methods of single-channel parallel PID and fuzzy adaptive PID control, dual-channel cross-coupling PID and fuzzy PID compound control were selected to control the vehicle of tracked tobacco harvester to walk in a straight line. Each control method performs three straight-line walking modes: forward, acceleration and deceleration. The schematic diagram of the test site is shown in Figure 7. The test site selects the hard road surface in Zhengzhou Xindafang Industrial Park, and prepares double-sided tape, tape, GNSS receiver and its supporting devices as measuring instruments and equipment.

**Fig. 7 - Straight driving test of tobacco harvester**

During the test, the tobacco harvester was aligned parallel to the yellow line on the ground. The starting point for the driving test was determined at the intersection of a straight line perpendicular to the yellow line (marked with double-sided tape) and the frontmost and outermost contact point of the tracked tobacco harvester. The distance between this contact point and the yellow line was measured.

The harvester then traveled 100 meters along the yellow line. The endpoint was established and marked in the same manner as the starting point. During the straight-line driving test, except for the acceleration and deceleration phases, the driver did not perform any operations on the tracked tobacco harvester. Upon reaching the endpoint, the lateral deviation distance was measured using a tape measure. The deviation was recorded as negative when to the left and positive when to the right. The formula for calculating the yaw rate is:

$$\xi = \frac{|\Delta s|}{s} \times 100\% \quad (8)$$

where: $\xi$ - offset rate, %;

$\Delta s$ - deviation, m;

$s$ - calibrated travel distance, m.

During the straight-line running tests of the tobacco harvester, the output speed of the travel motors on both sides was set to 50 r/min, resulting in a forward speed of approximately 1.33 m/s for the harvester. When testing acceleration and deceleration, the speed of the travel motors on both sides was adjusted by ±20 r/min midway through the test. To avoid excessive system impact affecting straight-line performance, the controller sent a ramp signal with an action time of 2 seconds. The corresponding forward speeds of the harvester during these phases were 1.86 m/s and 0.80 m/s, respectively. Three sets of data were collected for each test condition. The test deviation records are presented in Table 3.

**Table 3**

**Straight-line driving test results of tobacco harvester**

| Test data | Non-cross coupled PID | | | Non-coupled fuzzy PID | | | Cross-coupled PID | | | Cross-coupled fuzzy PID | | |
|---|---|---|---|---|---|---|---|---|---|---|---|---|
| | constant | acceleration | deceleration | constant | acceleration | deceleration | constant | acceleration | deceleration | constant | acceleration | deceleration |
| Deviation $\Delta S_1$/m | 4.16 | 6.68 | 6.18 | 4.08 | 6.38 | 5.32 | 3.54 | 5.11 | 4.67 | 3.38 | 4.88 | 4.17 |
| Deviation $\Delta S_2$/m | 4.09 | 6.88 | 6.33 | 4.11 | 6.44 | 5.53 | 3.51 | 5.15 | 4.71 | 3.27 | 4.72 | 4.32 |
| Deviation $\Delta S_3$/m | 4.14 | 6.81 | 6.15 | 4.06 | 6.33 | 5.36 | 3.58 | 5.22 | 4.77 | 3.17 | 4.81 | 4.28 |
| Average yaw rate $\xi$/% | 4.13 | 6.79 | 6.22 | 4.09 | 6.39 | 5.41 | 3.55 | 5.16 | 4.72 | 3.27 | 4.84 | 4.26 |

***Steering Performance Test of Tracked Tobacco Harvester***

Steering performance is an important indicator for evaluating the rationality of the power drive system and the structural layout of a tracked vehicle. As noted above, tracked-vehicle steering can be classified into two modes according to the steering radius: R≥B/2 and 0≤R<B/2. To compare the effects of the two control algorithms on the harvester's steering performance, the left and right travel motor speeds, the relative error of the steering radius, and the track slip and slip ratio were evaluated and analyzed.

***Rotational Speed Analysis of the Bilateral Travel Motors***

When the turning radius of the tobacco harvester is R ≥ B/2, the rotational speed of the inner travel motor is set to 20 r/min, while that of the outer travel motor is 35 r/min. Under this condition, the harvester performs a large-radius differential steering maneuver. When the turning radius of the tobacco leaf harvester is 0 ≤ R < B/2, the inner travel motor rotates at 35 r/min, whereas the outer travel motor rotates at – 35 r/min, enabling the harvester to execute an in-place turning maneuver. The speed acquisition method for both motors is identical to that used in the straight-line driving tests. The encoder-based speed measurement resolution is 0.1 r/min, and the sampling frequency is set to 2 Hz. The corresponding results are presented in Table 4.

Table 4

**Speed parameters of the two hydraulic travel motors during steering tests**

| Parameter | | Differential steering | | Pivot steering | |
|---|---|---|---|---|---|
| | | Inner motor | Outer motor | Inner motor | Outer motor |
| Theoretical value (r·min$^{-1}$) | | 20 | 35 | 35 | -35 |
| PID control | Average speed error | 0.86 | 0.70 | 1.20 | 1.22 |
| | Maximum speed error | 3.3 | 2.2 | 3.5 | 3.4 |
| Fuzzy PID control | Average speed error | 0.52 | 0.44 | 0.88 | 0.86 |
| | Maximum speed error | 2.6 | 1.7 | 2.8 | 2.8 |

$$\text{Average speed error} = \frac{|N_{out} - N_{in}|}{m} \quad (9)$$

As shown in Table 4, both control algorithms achieve satisfactory performance during the steering of the tracked tobacco harvester. However, the pump-controlled motor system under fuzzy PID control exhibits higher speed tracking accuracy, indicating that the fuzzy PID controller has superior adaptability to parameter variations and external load disturbances.

***Steering Trajectory and Offset Measurement***

The turning trajectory of a tracked vehicle is not as intuitive to observe as its straight-line trajectory. To accurately characterize the turning behavior of the crawler-type tobacco harvester, a GNSS receiver and its associated equipment were employed to collect real-time positional data, which were subsequently used to reconstruct and analyze the vehicle's travel trajectory. The UniStrong high-precision GNSS system used in this study is shown in Figure 8.

To facilitate observation of the rotational center offset during in-place turning, the mobile GNSS station was intentionally not installed at the geometric center of the tracked tobacco harvester. The installation position of the mobile station is illustrated in Figure 9, where points O and $O_1$ denote the geometric center of the harvester and the phase center of the mobile station, respectively. The horizontal distance $a$ between these two points was set to 0.5 m, and the installation height of the mobile station phase center was 2.8 m above the ground. Due to this elevated mounting position, vibrations generated during harvester operation could potentially affect the positioning accuracy. To evaluate the stability and reliability of the GNSS measurements, a fixed-point positioning test was conducted. Specifically, positional data were collected while the harvester remained stationary, yielding a total of 200 data points. After coordinate transformation and analysis, the data were found to be concentrated within a circular region of 1 cm radius, indicating that the positioning system maintained high measurement accuracy during operation. This level of precision satisfies the requirements of the experimental conditions. The test site is shown in Figure 10.


**Fig. 8 - UniStrong high precision GNSS RTK equipment**

*1. Antenna; 2. Controller; 3. Antenna; 4. Satellite radio*

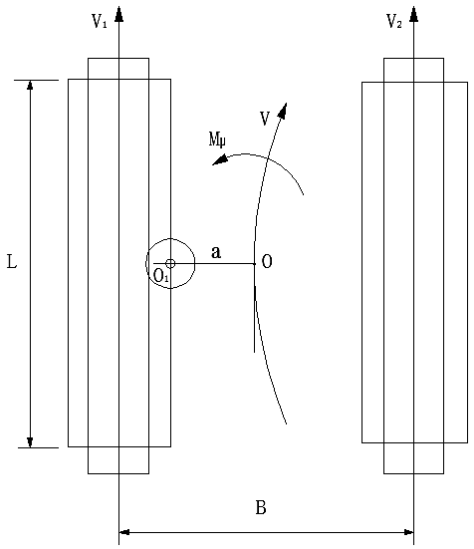


Fig. 9 - Schematic diagram of the installation of mobile station


Fig. 10 - Steering test site of Tobacco harvester

## RESULTS

### *Straight-Line Driving Test Procedure and Results Analysis*

1) Analysis of the Deviation Rate Results

At present, there is no specific industry standard for evaluating the straight-line driving performance of tobacco harvesters. Therefore, this study refers to the agricultural machinery standard DG/T 186–2019 (Ginger Harvester) as a reference. According to this standard, a deviation rate of no more than 6% was adopted as the evaluation criterion for the straight-line driving performance of the tobacco harvester. The experimental results indicate that, under cross-coupled synchronous control, the deviation rate of the tobacco harvester during uniform straight-line motion satisfies the stipulated requirement. Furthermore, compared with conventional PID control, the fuzzy adaptive PID controller effectively reduced the average deviation rate under all three straight-line driving conditions (uniform speed, acceleration, and deceleration). These results demonstrate that fuzzy PID control exhibits superior disturbance rejection capability compared with traditional PID control, thereby confirming the effectiveness and practicality of the cross-coupled composite synchronous control strategy. When cross-coupled synchronous control was not applied, the deviation rates obtained under both control algorithms during uniform straight-line driving met the evaluation criterion and were numerically close, indicating satisfactory performance. This observation reflects the inherent robustness of conventional PID control in linear systems. However, during accelerated straight-line driving, only the deceleration condition under fuzzy adaptive PID control satisfied the deviation criterion, whereas the acceleration condition failed to meet the requirement.

2) Analysis of the Speeds of the Dual-Sided Travel Motors

Using the data storage function of the control system, the speed signals of the two travel motors during the straight-line driving tests were recorded and imported into MATLAB for post-processing and analysis. The measured speed data were then compared with the corresponding reference (target) speed values. The speed signals were obtained from the incremental encoders installed on the hydraulic motors. Considering that the speed differences between the left and right travel motors during straight-line operation are relatively small, the encoder measurement resolution was set to 0.1 revolutions per minute (r/min), and the sampling frequency was configured as 2 Hz. The corresponding speed response curves and comparative results are presented in Figures 13–19.

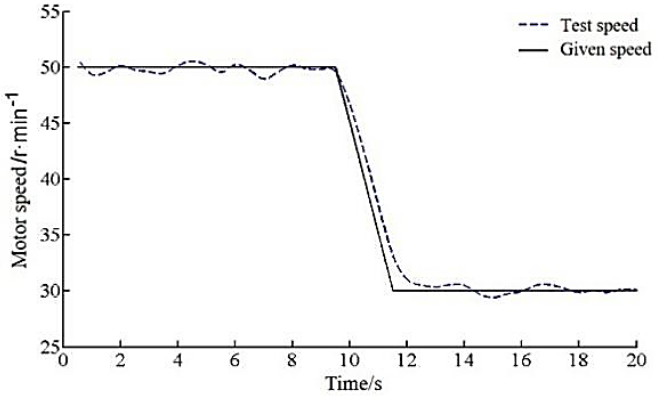


**Fig. 11 - Straight-line deceleration (PID)**

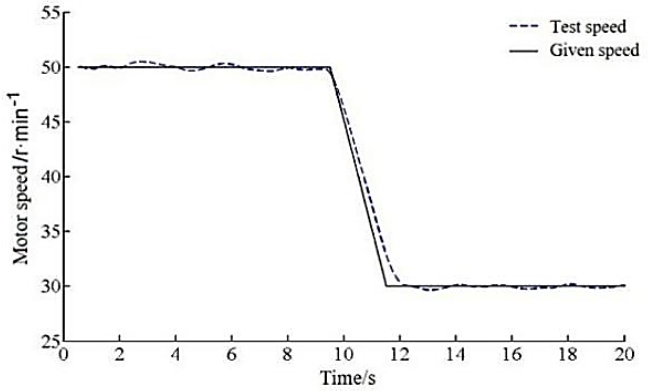


**Fig. 12 - Straight-line deceleration (Fuzzy PID)**

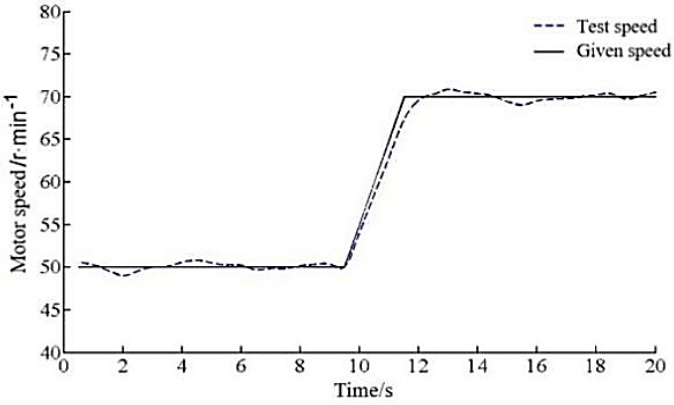


**Fig. 13 - Straight-line acceleration (PID)**

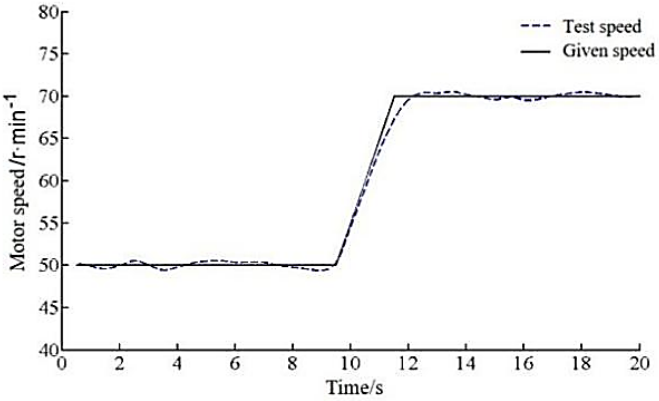


**Fig. 14 - Straight-line acceleration (Fuzzy PID)**

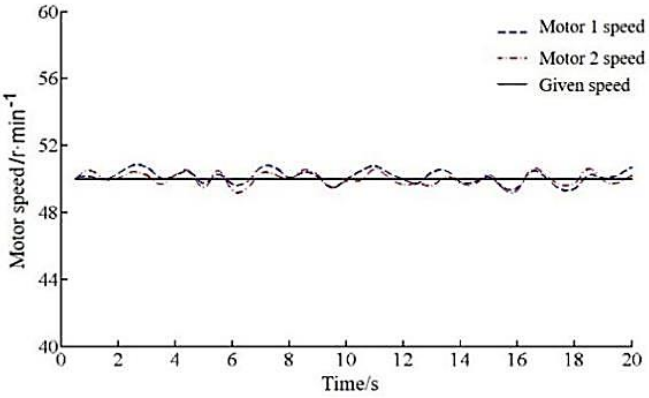


**Fig. 15 - Cross-coupled PID control**

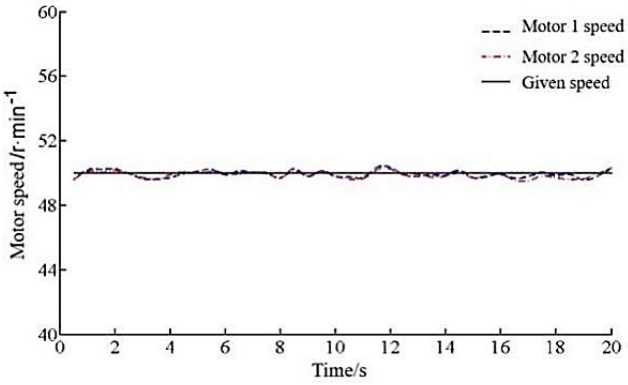


**Fig. 16 - Cross-coupled fuzzy PID control**

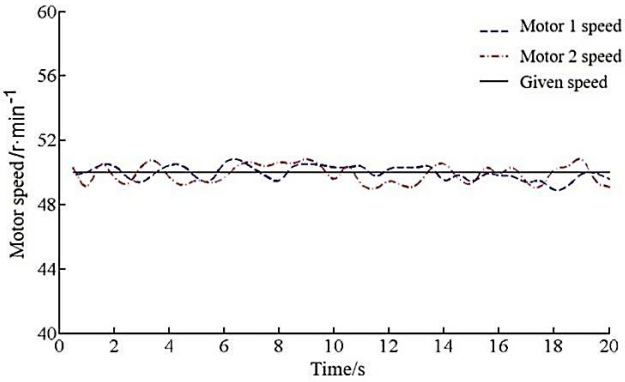


**Fig. 17 - Parallel PID control**

To facilitate a comparative analysis of the control performance of the fuzzy PID and conventional PID algorithms, the output speeds of the travel motors during straight-line acceleration and deceleration were extracted under both control strategies without cross-coupling. The corresponding results are presented in Figures 11–14. As shown in the figures, the output speeds of the left and right travel motors remain relatively stable under both control schemes. During straight-line acceleration and deceleration, the steady-state errors under conventional PID control were approximately ±1.3 r/min and ±1.0 r/min, respectively. In contrast, the steady-state errors under fuzzy PID control were reduced to ±0.7 r r/min and ±0.3 r/min, respectively. Moreover, the fuzzy PID controller exhibited smaller tracking errors in response to step inputs compared with the conventional PID controller. These results indicate that fuzzy PID control provides superior disturbance rejection capability and faster dynamic response, demonstrating improved robustness and adaptability to external load variations.

The effects of the cross-coupled synchronous composite control strategies are illustrated in Figures 15–17. When parallel PID control is applied to regulate the speeds of the dual-channel travel motors, the steady-state error of the system output speed is approximately ±1.3 r/min. Under this condition, the maximum and average speed differences between the two channels are ±1.5 r/min and ±0.7 r/min, respectively.

When the cross-coupled double closed-loop PID control strategy is employed, the steady-state error is reduced to ±0.9 r/min, while the maximum and average speed differences decrease to ±0.7 r/min and ±0.3 r/min, respectively. Furthermore, when the cross-coupled double closed-loop fuzzy PID control strategy is adopted, the steady-state error is further reduced to ±0.5 r/min, and the maximum and average speed differences between the two travel motors decrease significantly to ±0.2 r/min and ±0.11 r/min, respectively. These results demonstrate that the control performance follows the order: cross-coupled fuzzy PID > cross-coupled PID > parallel PID, indicating that the proposed cross-coupled fuzzy PID strategy provides the highest synchronization accuracy, strongest disturbance rejection capability, and best overall control performance.

***Steering Maneuver Test Results Analysis***

During the steering tests, when the turning radius of the tobacco harvester satisfied R ≥ B/2, the speed of the outer travel motor was set to 35 r/min, while that of the inner travel motor was set to 20 r/min. Under this condition, the corresponding linear speeds of the outer and inner tracks were 0.93 m/s and 0.53 m/s, respectively, resulting in a large-radius differential steering maneuver. When the turning radius satisfied 0 ≤ R < B/2 the outer travel motor speed remained at 35 r/min, while the inner travel motor speed was reversed to –35 r/min. In this case, the tobacco harvester executed an in-place pivot turn, with both tracks rotating at a linear speed of 0.93 m/s. The relationship between the turning radius of the track-grounding center on both sides of the tobacco harvester and the turning trajectory radius of the GNSS mobile station phase center is expressed by Equation (10).

$$R_{ni} = R_i + 0.5 \tag{10}$$

where: $R_{ni}$ -- the turning-trajectory radius of the phase center of the mobile station when the tobacco harvester is turning, m;

$R_i$ --the turning-trajectory radius of the harvester's ground geometric center during turning, m;

For $i$ = 1 and $i$ = 2, the two steering modes correspond to (1) a steering radius R ≥ B/2 and (2) a steering radius 0 ≤ R < B, respectively.

The position data (xi, yi), ($i$ = 1,2,3 · · ·) collected by GPS were processed and imported into MATLAB. A circle-fitting model was then established to estimate the turning trajectory. The steering trajectories under the two control methods are shown in Figures 18 and 19.

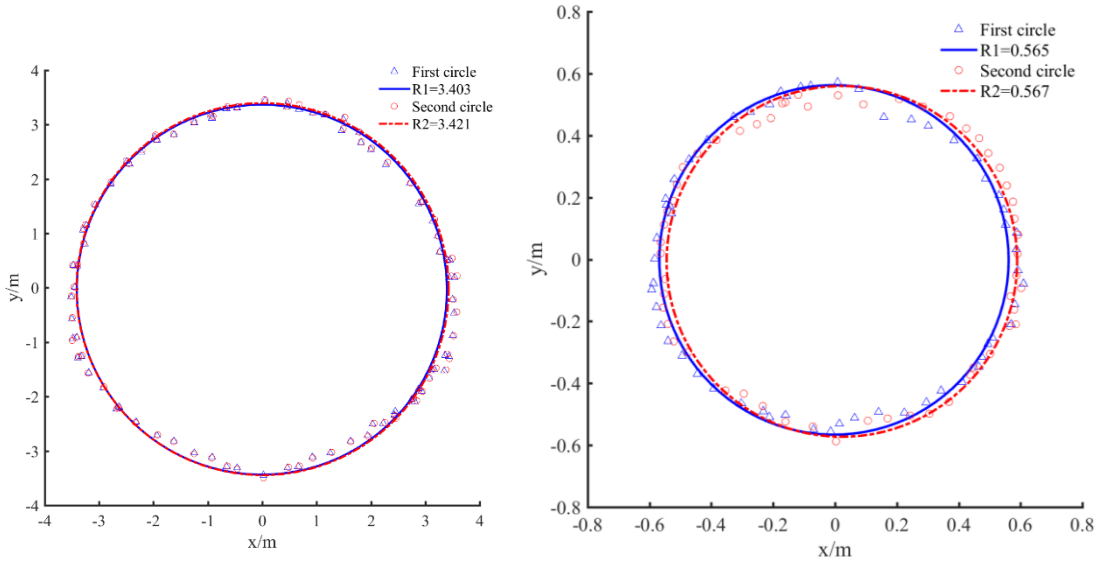


**(a) R≥B/2 Turning track** **(b) R<B/2 Turning track**

**Fig. 18 - Turning tracks of Tobacco harvester (PID)**

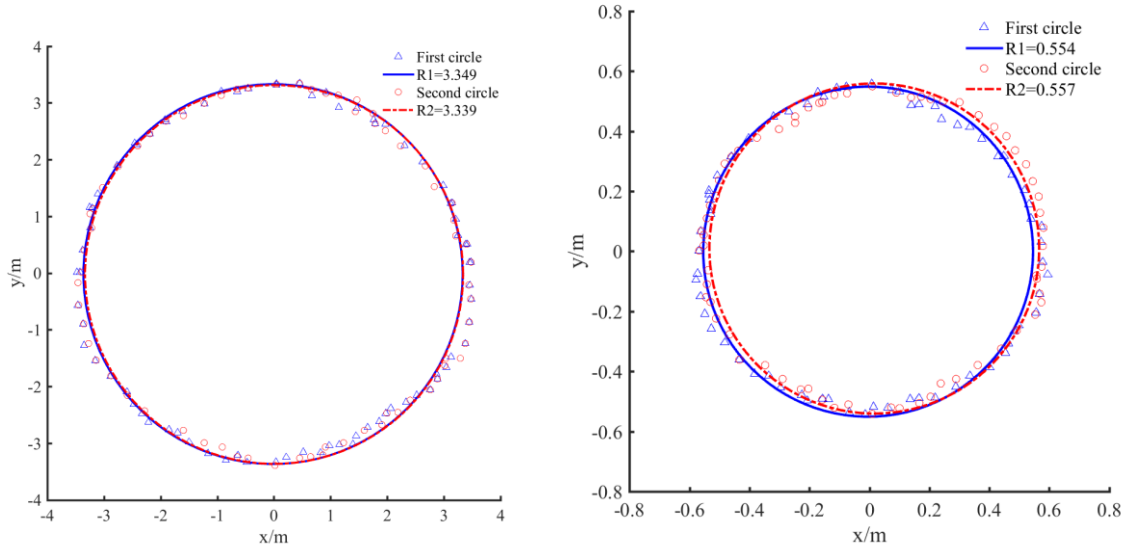


(a) R≥B/2 Turning track (b) R<B/2 Turning track

Fig. 19 - Turning tracks of Tobacco harvester (Fuzzy PID)

Table 5

Turning parameters of the tobacco harvester under PID control

| Steering type | Turning track number | Trajectory radius of the receiver phase center | | | Trajectory radius of the frame geometric center | | | |
|---|---|---|---|---|---|---|---|---|
| | | Circle center abscissa / m | Circle center ordinate / m | Radius / m | Value of each group / m | Average / m | Theoretical value / m | Relative error |
| R≥B/2 | 1 | -0.001 | -0.034 | 3.403 | 2.903 | 2.912 | 2.68 | 7.3% |
| | 2 | 0.005 | -0.024 | 3.421 | 2.921 | | | |
| 0≤R<B/2 | 1 | -0.004 | -0.002 | 0.565 | 0.065 | 0.066 | 0 | 13.2% |
| | 2 | 0.022 | -0.007 | 0.567 | 0.067 | | | |

Table 6

Turning parameters of the tobacco harvester under Fuzzy PID control

| Steering type | Turning track number | Trajectory radius of the receiver phase center | | | Trajectory radius of the frame geometric center | | | |
|---|---|---|---|---|---|---|---|---|
| | | Circle center abscissa / m | Circle center ordinate / m | Radius / m | Value of each group / m | Average / m | Theoretical value / m | Relative error |
| R≥B/2 | 1 | -0.015 | -0.020 | 3.349 | 2.849 | 2.844 | 2.68 | 5.16% |
| | 2 | -0.003 | -0.027 | 3.339 | 2.839 | | | |
| 0≤R<B/2 | 1 | -0.042 | -0.001 | 0.554 | 0.054 | 0.056 | 0 | 11.2% |
| | 2 | 0.016 | 0.009 | 0.557 | 0.057 | | | |

Tables 5 and 6 present the steering trajectory parameters obtained under the two control methods. By comparing the steering trajectories, it can be observed that the tracked tobacco harvester achieves satisfactory steering performance under both control algorithms. Under fuzzy PID control, the average turning radii of the geometric center of the tracked vehicle are 2.844 m and 0.056 m for the two steering modes, with corresponding relative errors of 5.16% and 11.2%, respectively. Under conventional PID control, the average turning radii are 2.912 m and 0.066 m, with relative errors of 7.3% and 13.2%, respectively. According to the experimental results, the relative error of the steering radius under fuzzy PID control is approximately 2% lower than that under conventional PID control for both steering modes, indicating that the fuzzy PID algorithm provides higher steering accuracy.

## CONCLUSIONS

To meet the operational requirements of the tracked tobacco harvester in hilly tobacco fields, a dual pump-dual motor hydraulic drive system was designed. A fuzzy PID control method was adopted to regulate the speed of the single-channel pump-controlled motor system. To address the challenge of synchronous control during both straight-line motion and steering, a cross-coupled dual closed-loop synchronous control strategy was proposed, along with an internal deceleration differential steering mechanism. These methods enable precise control of the harvester's linear motion and steering behavior.

During straight-line driving, the steady-state error of the system output under conventional PID control was ±1.3 r/min and ±1.0 r/min, whereas under fuzzy PID control, the error was reduced to ±0.7 r/min and ±0.3 r/min, respectively. Moreover, fuzzy PID exhibited superior performance in tracking the slope of the response curve, demonstrating its advantages over conventional PID in terms of output stability and response speed. Under parallel PID control, the steady-state error of the system output speed was ±1.3 r/min, accompanied by a relatively large speed difference between the two motor channels. With dual closed-loop PID control, the steady-state error decreased to ±0.9 r/min, and the inter-channel speed difference was correspondingly reduced. Under dual closed-loop fuzzy PID control, the steady-state error was further reduced to ±0.5 r/min, with the smallest speed difference observed among all control strategies. In turning driving tests, the average turning trajectory radius under fuzzy PID control was 2.844 m, with a relative error of 0.056 m, both of which were lower than those under conventional PID control (2.912 m and 0.066 m, respectively). In addition, the slip rates under fuzzy PID control were consistently lower than those under PID control. These results demonstrate that fuzzy PID control provides superior performance in turning operations, characterized by smaller tracking errors, improved synchronization, and reduced speed differences.

Considering the complex operating environment encountered during tobacco leaf harvesting, future work could focus on integrating additional sensors, such as satellite antennas and feeler rods, into the tracked tobacco harvester. Based on real-time position and heading information, the controller could dynamically adjust the displacement of the variable-displacement pumps on both sides of the tracks. Combined with the current single-channel control strategy, this approach would enable real-time directional correction of the harvester. Ultimately, this would facilitate the realization of fully unmanned operation of the tracked tobacco harvester during field operations.

## ACKNOWLEDGEMENT

This study is supported by Henan Provincial Science and Technology Research Project (222102110457, 252102110365, 252102111171); Henan Tobacco Company Science and Technology Special (2023410000240029); Henan Provincial Postdoctoral Funding Project (279456); China National Tobacco Corporation tobacco agricultural machinery research project (110202301010); State key laboratory of intelligent agricultural power equipment open project "Hydraulic control system design of hydraulic drive track-laying vehicle"(SKLIAPE 2024011).

## REFERENCES

[1] Cao Y., Li Q.M., Wu G.Q. (2023). Research Progress of Hydraulic Synchronous System (液压同步系统研究进展). *Modern Manufacturing Engineering*.Vol.11, pp.136-140, Beijing/China.

[2] Duan Z., Sun C., Li J. (2024). Research on servo valve-controlled hydraulic motor system based on active disturbance rejection control. *Measurement and Control.* Vol.57, pp.113-123, New York/USA.

[3] Fang Z., Huang C.L., Xu Y.S., Zhang C.M. (2020). Research on closed-loop control system for friction welding machine moving velocity based on PID (基于 PID 算法摩擦焊机移动速度闭环控制系统研究). *Machine Tool & Hydraulics.* Vol.48, pp.29-36, Guangzhou/China.

[4] Fu S., Li Z., Lin T., Chen Q. (2020). A positive flow control system for electric excavators based on variable speed control. *Applied Sciences.* Vol.10, pp.4826, Basel/Switzerland.

[5] Helian B., Chen Z., Yao B., Chenl. (2020). Accurate motion control of a direct-drive hydraulic system with an adaptive nonlinear pump flow compensation. *IEEE/ASME Transactions on Mechatronics.* Vol.26, pp.2593-2603, Haerbin/China.

[6] Liao L., Xiang G., Zheng X., Zhu Y., Xiao Q., Dian S. (2023). Synchronous Control of Parallel-Hydraulic System Based on Linear Active Disturbance Rejection (基于线性自抗扰的并联液压系统同步控制). *Modular Machine Tool & Automatic Manufacturing Technique.* Vol.5, pp.60-63, 68, Dalian/China.

[7] Liu Z.L., Liu M.Q., Wang J.M., Wang Z.M. (2022). Design and simulation of pile leg synchronous control system for jack-up wind turbine installation ship (自升式风电安装船桩腿同步控制系统的设计与仿真). *Machine Tool & Hydraulics.* Vol.20, pp.113-117, Guangzhou/China.

[8] Lu S., Wang H., Zhao G., Zhou G. (2023). Grey wolf particle swarm optimized pump–motor servo system constant speed control strategy. *Machines.* Vol.11, pp.178, Basel/Switzerland.

[9] Ly L., Chen Z., Yao B. (2020). Advanced valves and pump coordinated hydraulic control design to simultaneously achieve high accuracy and high efficiency. *IEEE Transactions on Control Systems Technology.* Vol.29, pp.236-248, USA.

[10] Nguyen M.H., Ahn K.K. (2023). Output feedback robust tracking control for a variable-speed pump-controlled hydraulic system subject to mismatched uncertainties. *Mathematics.* Vol.11, pp.1783, Basel/Switzerland.

[11] Pascal M.A., Aly A.A.E., Taher R. (2020). Nonlinear PID actuator speed control in inverter based electro-hydraulic systems subjected to external leakage. *Australian Journal of Mechanical Engineering*. Vol.18, pp.443-454, Australia.

[12] Ranjan P., Wrat G., Bhola M., et al. (2020). A novel approach for the energy recovery and position control of a hybrid hydraulic excavator. *ISA Transactions.* Vol.99, pp.387-402, New York/USA .

[13] Ren H., Li W., Ye S., Xu B. (2023). Design of visual navigation system for agricultural robots based on PID-fuzzy control and monocular vision. *INMATEH - Agricultural Engineering.* Vol.70, pp.117-126, Bucharest/Romania .

[14] Ren Q. (2020). Intelligent control technology of agricultural greenhouse operation robot based on fuzzy PID path tracking algorithm. *INMATEH - Agricultural Engineering.* Vol.62, pp.181-190, Bucharest/Romania .

[15] Senthilkumar P., Sivakumar K., Kanagarajan R., Kuberan S. (2018). Fuzzy control of active suspension system using full car model. *Mechanika*. Vol.24, pp.240-247, Kaunas/Lithuania.

[16] Shen W., Wang J. (2022). An integral terminal sliding mode control scheme for speed control system using a double-variable hydraulic transformer. *ISA Transactions.* Vol.124, pp.386-394, New York/USA.

[17] Tian Q., Gu L. (2021). Instantaneous speed fluctuation extraction and its application for efficiency evaluation of hydraulic system. *Australian Journal of Mechanical Engineering.* Vol.19, pp.356-362, Melbourne/Australia.

[18] Wang F., Wu J., Lin Z., Zhang H. (2023). A power-sharing electro-hydraulic actuator system to downsize electric motors for electric mobile machines. *Energy.* Vol.284, pp.129343, England.

[19] Wang J., Liu Z., Chen H., Zhang Y. (2023). Trajectory tracking control of a skid-steer mobile robot based on nonlinear model predictive control with a hydraulic motor velocity map. *Applied Sciences.* 14(1): 122. Vol.14, pp.122, DOI: 10.3390/app14010122 Basel/Switzerland.

[20] Wang Y.F., Ding H.G., Zhao J.Y., Li R. (2022). Neural network-based output synchronization control for multi-actuator system. *International Journal of Adaptive Control*.Vol.36, pp.1155-1171, Chichester, West Sussex/England.

[21] Wrat G., Bhola M., Ranjan P., Mishra S. (2020). Energy saving and Fuzzy-PID position control of electro-hydraulic system by leakage compensation through proportional flow control valve. *ISA Transactions.* Vol.101, pp.269-280, New York/USA.

[22] Xie J.H., Tang G.Y., Huang D.M. (2013). Modeling and simulation optimization of dual-motor synchronous drive position servo system (双电机同步驱动位置伺服系统的建模与仿真优化). *Machinery & Electronics.* Vol.1, pp.22-25, Guizhou/China.

[23] Zhang X., Zhang J., Han M., Fang Y. (2023). Design and Optimization of Self-Compensation Oil Distributor for Hydraulic Motors. *IEEE/ASME Transactions on Mechatronics.* Vol.29, pp.2103-2114, Piscataway/USA.

[24] Zhao L.Z., Su D.H., Zuo W., Zou H.T. (2022). Synchronous control system of hydraulic cylinder of fan coil car controlled by particle swarm fuzzy PID. *Journal of Mechanical & Electrical Engineering*. Vol.39, pp.961-966, Zhenjiang/China.